Contents lists available at ScienceDirect

Food Chemistry: Molecular Sciences

Transcriptome analysis reveals the potential mechanism of polyethylene packing delaying lignification of *Pleurotus eryngii*

Wancong Yu [a,1], Shihao Li [b,1], Bowen Zheng [b], Yuqi Wang [c], Yue Yu [b], Yumeng Wang [b], Xu Zheng [b], Jiping Liu [d], Zhijun Zhang [e,*], Zhaohui Xue [b,*]

[a] Biotechnology Research Institute, Tianjin Academy of Agricultural Sciences, 300384 Tianjin, China
[b] School of Chemical Engineering and Technology, Tianjin University, Tianjin 300072, China
[c] School of Environmental Science and Engineering, Guangzhou University, Guangzhou 510006, Guangdong, China
[d] Robert Holley Center, US Department of Agriculture, Agricultural Research Service, Cornell University, Ithaca, NY 14853, USA
[e] National Engineering Technology Research Center for Preservation of Agricultural Products, Tianjin Key Laboratory of Postharvest Physiology and Storage of Agricultural Products, 300384 Tianjin, China

A B S T R A C T

Transcriptome analysis is important for the quality improvement of edible fungi, however, the effect of polyethylene (PE) packaging on the preservation of *Pleurotus eryngii* at the transcriptome level still needs to be further investigated. In order to elucidate the effect of PE on delaying lignification of *P. eryngii*, this study focused on exploring effects of PE on enzymes and genes involved in lignification. The results showed that PE packaging delayed the deterioration of phenotype, color difference and weight loss rate of *P. eryngii*, inhibited lignin and H_2O_2 content and maintained firmness and cellulose content. The activities of PAL, POD, 4-CL were inhibited, and more laccase expression was activated. Fifty-five differentially expressed genes associated with laccase, multifunctional peroxidase (VP), POD and 4-CL were screened from 10 d, 20 d and 30 d transcriptome data. These results show that PE could inhibit lignification of *P. eryngii* by up-regulating laccase and VP related genes involved in lignin decomposition and down-regulating the expression of genes involved in lignin synthesis. Meanwhile, we employed Confocal Raman microspectroscopy (CRM) to realize lignin cell level visualization and PE could reduce lignin deposition and weaken the lignin signal bands formed. Therefore, PE can alleviate the lignification of *P. eryngii* during storage by regulating the expression of specific genes, advancing the understanding of lignification in postharvest *P. eryngii* at the molecular level, and CRM has the potential to detect the changes of *P. eryngii* cell wall.

1. Introduction

Pleurotus eryngii belongs to Pleurotaceae, Agaricomycotina, Basidiomycota, Fungi. *P. eryngii* contains various bioactive substances such as terpenoids, sterols, polysaccharides and polyphenols, which can be developed into natural and functional foods and drugs to resist reactive free oxygen species, delay the aging process, and improve postprandial blood glucose (Kleftaki et al., 2022; Zhang et al., 2021). The post-harvest physiological state of *P. eryngii* is susceptible to various environmental factors, including temperature, humidity, gas environment and other microbial community infections. Therefore, storage technologies for edible mushrooms are of great interest, including low-temperature storage, gas packaging, irradiation, ozone, pressure-reducing treatment, and reagent preservation. (Shekari et al., 2021).

In practical application, low-temperature storage is a key strategy to maintain the commodity quality of *P. eryngii* after harvest due to cost considerations (Nie et al., 2020). However, the suitable temperature for *P. eryngii* growth environment is 24 °C-27 °C. Long-term storage at low temperature may induce chilling injury and lead to metabolic disorder and lignification (Zhang et al., 2021). Lignification is considered to be a response to abiotic stress, a process in which lignin monomers are synthesized in large quantities and polymerized to form lignin macromolecules deposited on the cell wall, accompanied by a series of secondary metabolic reactions(Cesarino, 2019). Numerous studies on postharvest lignification have focused on the activities of key enzymes in the

---

* Corresponding authors.
  E-mail addresses: tjzhangzj@sina.cn (Z. Zhang), zhhxue@tju.edu.cn (Z. Xue).
[1] Wancong Yu and Shihao Li contributed equally to this work.

Nomenclature

Abbreviations

TPA	Texture Profile Analysis
PAL	Phenylalanine Ammonia-Lyase
POD	Peroxidase
4-CL	4-Coumarate: Coa Ligase
ABTS	2,2′-Azino-Bis (3-Ethylbenzothazo-6-Sulfonate)
GO	Gene Ontology
KEGG	Kyoto Encyclopedia of Genes And Genomes
GAPDH	Glyceraldehyde 3-Phosphate Dehydrogenase
PE	Polyethylene
DEG	Differentially Expressed Gene
BP	Biological Processes
CC	Cell Components
MF	Molecular Functions
LiP	Lignin Peroxidase
MnP	Manganese Peroxidase
PCD	Programmed Cell Death
ROS	Reactive Oxygen Species
CRM	Confocal Raman microspectroscopy

phenylpropanoid pathway: phenylalanine ammonia-lyase (PAL), CAD, 4-CL and POD (Suo et al., 2018; Wen et al., 2020). Correspondingly, the biodegradation of lignin has also attracted extensive attention. The biodegradation of lignin in basidiomycetes has been reported to be initiated by single-electron oxidation and mediated by ligninolytic enzymes, including lignin peroxidase (LiP), VP and laccase (Zhuo and Fan, 2021). However, the current analysis of lignolytic enzyme lines contained by *P. eryngii* is not systematic enough.

PE and new nano-packaging materials developed on this basis have been proved to be able to inhibit lignification of mushrooms after harvest. Jiang et al. (2010) made modified atmosphere packaging (MAP) with 0.04 mm PE packaging and observed the effect of packaging on quality change of *Agaricus bisporus* stored at 4 °C. The results showed that firmness of mushroom was positively correlated with the accumulation of lignin. Compared with the unsealed control group, MAP treatment can reduce lignification process by inhibiting POD activity and lignin accumulation. Zuo et al. (2021) prepared nano PM and found that nano PM reduced lignin deposition by inhibiting PAL, C4H and 4-CL activities involved in phenylpropane pathway.

Transcriptome has been widely used to analyze the functional genes and molecular mechanisms related to the growth and development of edible fungi, including *Agrocybe aegerita, Cordyceps militaris* and *Ganoderma lucidum* (Hassan et al., 2020; Xu et al., 2021). In recent years, the transcriptomic research on fruit and vegetable lignification has been gradually deepened. Hou et al. (2022) elucidated by the transcriptome that Lei bamboo shoots at low temperature may inhibit lignification by downregulating lignin biosynthesis genes, such as *PAL, CAD, C3H, HCT-like* genes. Through RNA-seq, Wu et al. (2021) identified differentially expressed genes involved in the lignification process in two walnut cultivars. The results showed that lignification was closely related to the genes of phenylpropanoid pathway and flavonoid pathway, including *COMT, CAD, POD, C4H, CCR* and *CHS*. At the same time, the expression levels of transcription factors such as MYB, NAC and LBD were significantly different between the two cultivars, which may be the reason for the difference in endocarp development and lignification between the two cultivars. Sun et al. (2021) found that NO treatment could inhibit the expression of *AePAL, AEC4H, AE4CL, AeCAD* to reduce lignin biosynthesis, thereby delaying the lignification process of cold storage okra pods. In addition, the changes of pod phenotype, lignin content, NO content, related enzyme activity and H_2O_2 content were consistent with the differential expression of related genes, it is suggested that NO may

play an important role in delaying the lignification of okra pods during cold storage. Most of the current transcriptomic studies on *P. eryngii* revolve around culture under light conditions, heavy metal stress, and the development of functional foods (Du et al., 2020; Q. Li et al., 2018; Teniou et al., 2022; Xu et al., 2021). Wang et al. (2020) observed the expression patterns of *PEPAL1, PE4CL1, PE4CL3* and *PePOD* in *P. eryngii* stored at 1 °C for 21 consecutive days, these results suggest that they may be the key genes involved in the two lignification of *P. eryngii*. Nevertheless, the process of mushroom lignification is influenced by multiple factors and involves multiple metabolic pathways. It is necessary to explore more target genes of PE materials that inhibit the lignification of *P. eryngii* from a transcriptomics perspective.

Confocal Raman microspectroscopy (CRM) is a novel label free chemical microscopy hyperspectral imaging technique. CRM has been applied to probe the composition and structure of plant cell walls in recent years. Li et al. (2021) successfully observed Raman peaks of important nutrients such as starch, sucrose and amino acids from lily scales using CRM and demonstrated that nutrients such as starch, sucrose, amino acids and ferulic acid can be evaluated by CRM. Chylinska et al. (2017)introduced CRM to assess changes in the spatial distribution of polysaccharides in the tri-cell junctions or cell corner regions of tomato cell walls and finally recorded The dynamics of cell wall degradation (mainly pectin polysaccharides) during tomato ripening was recorded. Szymanska-Chargot et al. (2016) obtained changes in the distribution of cell wall polysaccharides during apple fruit development and senescence with the help of CRM and found that pectin in intermediate lamellae and primary cell walls is degraded, while changes in cellulose and hemicellulose were not significant. distribution changes and found degradation of pectin in intermediate lamellae and primary cell walls, while changes in cellulose and hemicellulose were not evident. Therefore the introduction of CRM to visualize cell wall components such as lignin changes over time and space at the single cell level would help facilitate the understanding of important postharvest fruit composition and quality changes.

In this study, we observed the effect of two PE films (0.02 mm, 0.05 mm) on the quality of *P. eryngii* during storage and analyzed the changes in enzyme activity associated with lignification. Transcriptome sequencing was performed at 10 d, 20 d and 30 d. Gene Ontology (GO) and Kyoto Encyclopedia of Genes and Genomes (KEGG) enrichment analysis were used to describe the regulatory pathway of PE on *P. eryngii*. In addition, CRM was used to monitor the changes in the spatial distribution of lignin in the cell wall of *P. eryngii*. Therefore, the present study was devoted to reveal the mechanism of PE regulation of lignification in *P. eryngii*.

2. Materials and methods

2.1. Mushroom treatment and storage

P. eryngii was harvested from Zhongyan Mushroom Co., Ltd., China on March 22, 2021. *P. eryngii* with uniform size (stipe length 17 ± 0.5 cm, stipe diameter 5 ± 0.5 cm), no mechanical injury or disease were picked and immediately transported to the laboratory and pre-cooled at low temperature at 8 °C for 12 h. *P. eryngii* was then randomly divided into 21 groups with 300 g in each group. PE film is provided by National Preservation Engineering Center, China. 0.02 mm and 0.05 mm polyethylene film were cut into 20 cm × 30 cm sizes.

Then *P. eryngii* were divided into three storage treatments: (1) directly stored in ZYLH-S80 incubator (Sinordc, China) with temperature of 4 °C and humidity of 90% RH (control); (2) packed in 0.02 mm PE bags, sealed with BSE-5038 heat sealer (ShouChuang, China), stored at 4 °C and 90% RH; (3) packed in 0.05 mm PE bags, sealed and stored at 4 °C and 90% RH. The firmness and springiness of each treatment group were analyzed every 5 d. At the same time, the stipe was fully frozen in liquid nitrogen and stored at −80 °C for subsequent measurement. The sampling time lasted for 30 d in total, and three replicates of each group

were analyzed every 5 d.

2.2. Measurement of appearance color and weight loss rate

The determination of surface color of *P. eryngii* with reference to Wang et al. (2019). L*, a* and b* values were measured with a Minolta Chromameter (Konica Minolta, Japan). The total color difference (ΔE) is calculated by the following equation:

$$\Delta E = \sqrt{\Delta L^{*2} + \Delta a^{*2} + \Delta b^{*2}}$$

where, ΔL* is difference in lightness and darkness, Δa* is difference in red and green, Δb* is difference in yellow and blue.

Before the start of low temperature storage, samples were randomly selected from each group of Abalone mushrooms, weighed to obtain the pre-storage mass and stored separately. After that, the samples were taken out and weighed to obtain the mass at the time of measurement at each sampling, and the weight loss rate was calculated and the results were averaged.

2.3. Firmness, cellulose, lignin and H_2O_2 determination

Firmness analysis were carried out with TA-XT plus texture analyzer (SMS, UK). The puncture experiment refers to Min et al. (2021) with appropriate modifications, The probe diameter was 2 mm, the pre-test velocity, test velocity and post-test velocity were 2 mm/s, the test distance was 5 mm. The parameter obtained is firmness, expressed in N. The middle part of stipe was taken for examination.

Cellulose content was determined using the plant tissue cellulose assay kit (Even Bridge Biotechnology, China) according to the manufacturer's instructions. The cellulose content was expressed as mg g^{-1}, and three parallel experiments were carried out in each treatment group.

The lignin determination method is referenced Huang et al. (2019) and modified. 1.0 g *P. eryngii* was homogenized in 5 mL 95 % ethanol and centrifuged (10000 g, 4 °C, 10 min). The precipitates were washed three times with ethanol and n-hexane. The dried product was dissolved in 2 mL 25 % brominated acetyl-glacial acetic acid solution. Centrifuged after incubation at 70 °C for 30 min and measured the light absorption value at 280 nm, the lignin content was expressed as A280 g^{-1}.

1.0 g *P. eryngii* was homogenized in 5 mL 5% TCA and centrifuge (10000 g, 4 °C, 15 min). To 1 mL supernatant, 1 mL potassium phosphate buffer (0.1 M, pH 7.6) and 1 mmol L^{-1} KI solution were added and mixed. The absorbance value was measured at 390 nm, and the H_2O_2 content in each g sample was expressed in $\mu mol \cdot g^{-1}$.

2.4. Enzyme activity assay

PAL, POD, 4-CL and laccase activities are determined in accordance with the assay kit instructions (Jiancheng, China). PAL activity was determined by L-Phenylalanine method. The absorbance at 290 nm was observed and recorded at 0 and 1 h, respectively. The change of absorbance at 290 nm per hour was 0.01 as a U. The activity of POD was determined by guaiacol method. The absorbance of the mixed solution within 180 s was recorded at 470 nm, with a rise of 0.01/min as a U. The activity of 4-CL was determined by p-coumaric acid method, and the absorbance at 333 nm was observed at 0 min and 5 min, respectively. A unit of 4-CL activity was defined as a 0.001 decrease in absorbance at 333 nm per minute. The laccase activity was determined by ABTS method. The amount of enzyme required for oxidation of 1 nmol ABTS per g of sample per minute was U. The activity values were expressed as 10^3 U kg^{-1}.

2.5. RNA-Seq sequencing and quantification of gene expression levels

Extraction of total RNA from *P. eryngii* was performed using TRIzol® reagent (Invitrogen, USA) according to the manufacturer's protocol.

mRNA was purified from total RNA using poly-T oligo-attached magnetic beads. The mRNA fragment was used as a template to synthesize cDNA and perform PCR. The library preparations were sequenced on an Illumina Novaseq platform (Novogene, China) and 150 bp paired-end reads were generated. Raw reads were submitted to the Sequence Read Archive (SRA) database (PRJNA789988, Accession Numbers SRR17267874–SRR17267900). Index of the reference genome was built using Hisat2 v2.0.5 and then paired-end clean reads were aligned to the reference genome.

Use featureCounts v1.5.0-p3 to calculate the number of reads mapped to each gene. And then FPKM of each gene was calculated based on the length of gene and reads count mapped to this gene. Differential expression analysis was performed on three biological replicates of each treatment using deseq2 R package. Differential expression in gene expression data was determined using a model based on negative binomial distribution. The resulting P-values were adjusted using the Benjamini and Hochberg's approach for controlling the false discovery rate. Genes with an adjusted P-value < 0.05 found by DESeq2 were assigned as differentially expressed.

2.6. GO and KEGG enrichment analysis

GO enrichment analysis of differentially expressed genes was implemented by the clusterProfiler R package. GO terms with corrected Pvalue<0.05 were considered significantly enriched by differential expressed genes. The clusterProfiler R package was used to perform statistical enrichment of differentially expressed genes in the KEGG pathway.

2.7. Validation of RNA-seq by quantitative real-time PCR

Ten genes were selected to verify the accuracy of expression profiling of RNA-Seq by qRT-PCR. The extracted RNA samples were treated with DNaseI and reversely transcribed into cDNA using the PrimeScript RT Reagent Kit with gDNA Eraser (Takara, China). All primers for qRT-PCR analysis were designed by Primer Premier 5.0 and listed in Supplementary Table S4. To normalize target gene expression, glyceraldehyde 3-phosphate dehydrogenase (*GAPDH*) was used as an internal reference. The relative gene expression level was calculated by $2^{-\Delta\Delta CT}$ method (Livak and Schmittgen, 2001).

2.8. Raman analysis

The tissues of *P. eryngii* were embedded in paraffin (Fallah-Joshaqani et al., 2021). Paraffin embedded tissues were prepared into 10 μm-thick slices and placed on aluminized glass sheets. All samples were covered with a layer of cover glass and sealed with nail polish. HR Evolution (HORIBA, Japan) is used for Raman signal acquisition. Excited by a 785 nm red laser, 600 notched grating, 50X long focal length. The N.A. value of the objective lens is 0.5 and the working distance is 10.5 mm. The step size of Raman imaging is set at 1 mm. The corresponding single point integration time is 30 s and the number of integration cycles is 2. The pinhole parameters are set at 100 μm to reduce the interference of the fluorescent background. The original Raman spectra were obtained and pretreated. By integrating the intensity within the Raman offset range defined in the baseline correction spectrum, the chemical image is calculated from two-dimensional (2D) and three-dimensional (3D) diagrams.

2.9. Statistical analysis

SPSS 26 software was used for statistical analysis, and quantitative detection datas in each group were expressed as mean ± standard deviation. T-test was used for comparison between two groups, one-way ANOVA analysis and Duncan multiple comparison were used for comparison between multiple groups. OriginPro 2018 was used for chart

preparation. Statistical data were considered significant when P < 0.05.

3. Results

3.1. Quality appearance and browning degree

Fig. 1A shows the phenotypic changes of *P. eryngii* during storage. From 0 to 5 d, the mushroom bodies of all groups were white, with full substrates and good sensory quality. After 10 d, yellow–brown patches gradually appeared on the surface of *P. eryngii* in CK group, and the tissues shrank due to dehydration. PE group maintained high quality during storage. At 30 d, PE group, especially 0.05 mm PE, still maintained well phenotype, which delayed the deterioration trend of quality.

The surface color difference of *P. eryngii* is shown in Fig. 1B. The color difference increases with the extension of storage time. At 30 d, the color difference was 41.51, 33.77 and 30.40 in CK, 0.02 mm and 0.05 mm PE groups, respectively, an increase of 29.36, 21.46 and 18.20 from the initial. At 20 d, the color difference of 0.02 mm group was 22% less than that of the control group (p < 0.01), while that of 0.05 mm group was 39% (p < 0.001). The weight loss rate of *P. eryngii* in different packages increased to different degrees (Fig. 1C). The weight loss rate of the control group of *P. eryngii* increased rapidly until 15 d, reaching 47.92% on 15 d. In contrast, 12.23 % weight loss was recorded in the 0.02 mm PE group on 30 d, and only 9.09 % in the 0.05 mm PE group on 30 d. This indicates that the PE packaging can control the moisture loss of *P. eryngii* during storage and effectively reduce the weight loss rate.

3.2. Firmness, cellulose, lignin and H_2O_2 content

As can be seen from Fig. 2A, the firmness increased and then decreased in all groups. During the whole storage period, the firmness of CK group reached two peaks (42.25 ± 1.06 N and 40.65 ± 1.14 N) at 10 d and 20 d, which increased by 37 % and 32 % respectively compared

with the initial. However, during 20–30 d, the firmness showed a sharp decline, especially decreased to 20.53 ± 1.07 N at 30 d. By contrast, the firmness of PE group was lower than CK group before 20 d. At 30 d, the firmness of 0.05 mm PE group was 27.28 ± 0.68 N, which was higher than CK group. The similar trend was found in 0.02 mm PE group. The firmness of PE group showed stronger stability during storage. As shown in Fig. 2B, the cellulose content of CK group was generally on the rise from 0 d to 20 d. Meanwhile, the cellulose content of the PE packaging group fluctuated slightly and was generally lower than that of CK group. In CK group, the cellulose degradation rate was further accelerated after 25 d, and the content was only 11.11 ± 0.71 mg g^{-1} at the end of storage, which was significantly lower than that of the PE-packaged group (p < 0.001). In contrast, the cellulose content of the PE-packed group, especially the 0.05 mm PE-treated group, fluctuated steadily from 20 d to 30 d and was still 22.63 ± 0.50 mg g^{-1} by 30 d.

As shown in Fig. 2C, the lignin content of the CK group increased 1.59-fold during storage, peaking at 10 d, 20 d and 30 d. The peak showed a gradual increase. With the progress of storage, PE group showed an inhibitory effect on lignin accumulation. At 10 d, the lignin content of 0.02 mm PE group and 0.05 mm PE group decreased by 17 % and 18 % respectively compared with CK group. After storage for 30 d, the inhibition rate reached 22 % and 31 %, which significantly alleviated the lignin content of *P. eryngii* during storage.

As shown in Fig. 2D, the initial H_2O_2 content of *P. eryngii* was 160.87 μmol g^{-1}. Within 30 d after storage, all treatment groups showed an increasing trend, and the H_2O_2 content in 0.02 mm PE and 0.05 mm PE was lower than that in the CK group (p < 0.05). The contents of H_2O_2 were 354.19, 269.73 and 234.28 in CK, 0.02 mm PE and 0.05 mm PE respectively, which were 2.20, 1.68 and 1.45 times of the initial value. The results showed that PE packaging treatment was beneficial to inhibit the increase of H_2O_2 content, and 0.05 mm PE performed better.
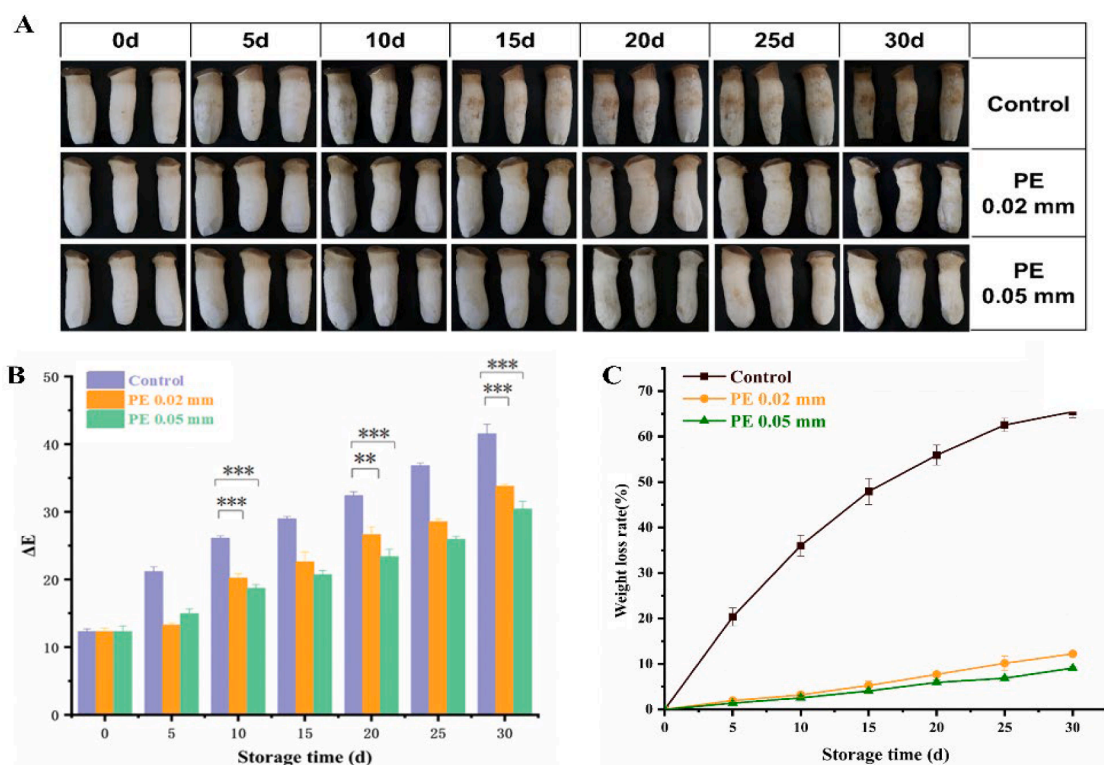

Fig. 1. Effect of PE on the (A) appearance quality, (B) color difference and (C) weight loss rate of *P. eryngii*. Data are presented as the means ± SD based on three independent experiments (*n* = 3). PE: polyethylene. * indicates the significant difference level between PE treatment group and CK group. *p < 0.05; **p < 0.01; ***p < 0.001.
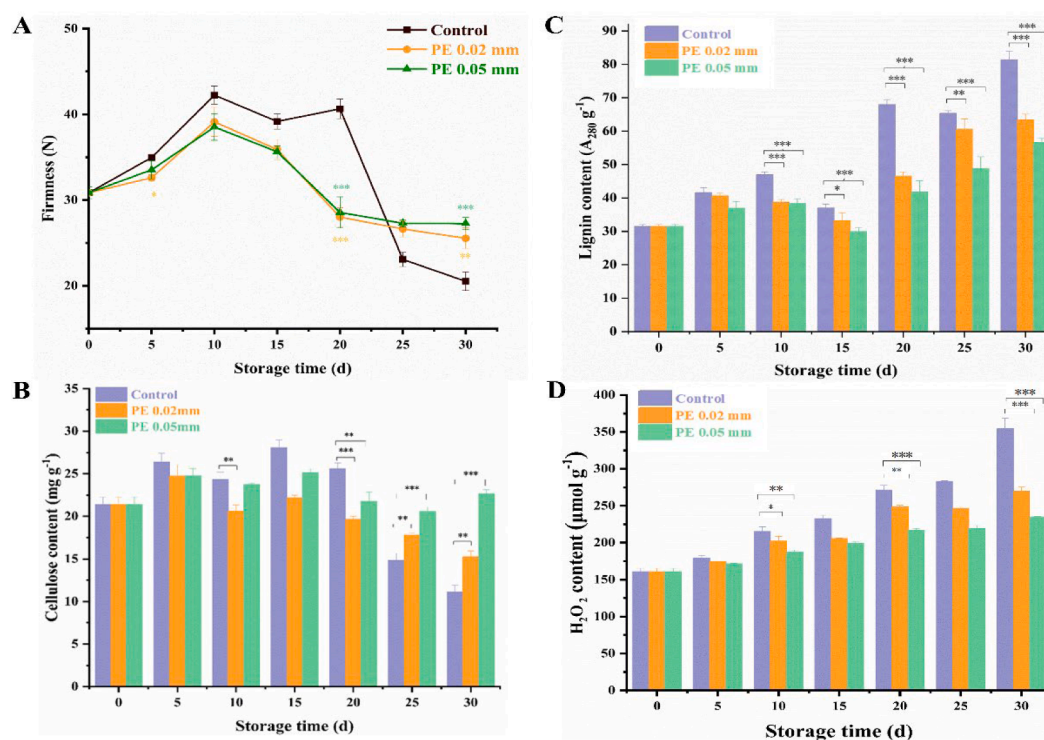
Fig. 2. Effect of PE on the (A) firmness, (B) cellulose content, (C) lignin content and (D) H_2O_2 content of *P. eryngii* during low temperature storage under different treatment. Data are presented as the means ± SD based on three independent experiments ($n = 3$). PE: polyethylene. * indicates the significant difference level between PE treatment group and CK group. *p < 0.05; **p < 0.01; ***p < 0.001.
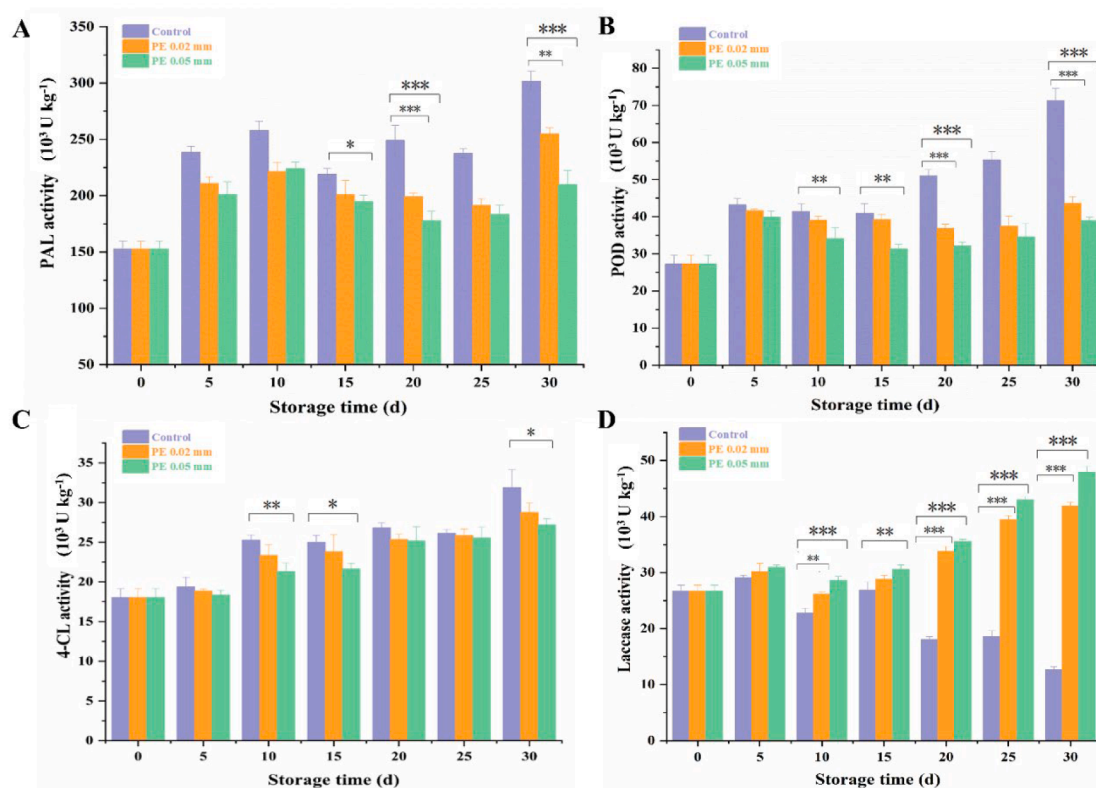

Fig. 3. Effects of PE packing on activities of (A) PAL, (B) POD, (C) 4-CL and (D)laccase of *P. eryngii* during storage. Data are presented as the means ± SD based on three independent experiments (n = 3). PE: polyethylene, PAL: phenylalanine ammonia-lyase, POD: peroxidase, 4-CL: 4-Coumarate: CoA ligase. * indicates the significant difference level between PE treatment group and CK group. *p < 0.05; **p < 0.01; ***p < 0.001.

3.3. PAL, POD, 4-CL and laccase activities

As shown in Fig. 3A, PAL activity in CK group showed a similar change trend to lignin, with three peaks throughout storage and an eventual increase of 98 %. At 15 d, the PAL activity in the 0.05 mm PE group was 194.62 ± 5.74 10^3 U kg^{-1}, which was 11% lower than that in CK group. The rise in PAL activity was inhibited by 29 % and 30 % at 20 d and 30 d, respectively. 0.02 mm PE treatment group inhibited PAL activity at 15 d, but not significant.

Low temperature storage directly after harvest elevated POD levels, especially after 20 d (Fig. 3B). The changes of POD in PE group fluctuated, and the ratio increased slightly. The increase of POD was inhibited by 39 % and 45 % at 30 d.

As for 4-CL activity, CK group continued to increase during storage and developed three peaks (Fig. 3C). At 30 d, the activity reached 31.87 ± 2.29 10^3 U kg^{-1}, which increased by 77 % compared with the initial value. Compared with CK group (25.28 ± 0.61 10^3 U kg^{-1}), the activity of 4-CL in 0.05 mm PE group was decreased at 10 d (21.30 ± 1.07 10^3 U kg^{-1}). At 15 d and 30 d, the high expression of 4-CL activity was also inhibited in 0.05 mm PE group. The 4-CL activity in 0.02 mm PE group was lower than CK group, but the trend was not significant.

In Fig. 3D, the activity of laccase in CK group decreased from 15 d. At 20 d and 30 d, the activity was 18.07 ± 0.48 10^3 U kg^{-1}, 12.65 ± 0.54 10^3 U kg^{-1}, only 68 %, 47 % of that at 0 d (26.71 ± 1.03 10^3 U kg^{-1}). In contrast, the PE and CK groups showed differences after 10 d, and the differences widened after 20 d. The laccase activity of 0.05 mm PE group reached 35.57 ± 0.39 10^3 U kg^{-1} and 47.91 ± 1.06 10^3 U kg^{-1} at 20 d and 30 d, which were higher than CK group.

3.4. Differentially expressed genes and enrichment analysis

To reveal the underlying mechanism by which PE material inhibits
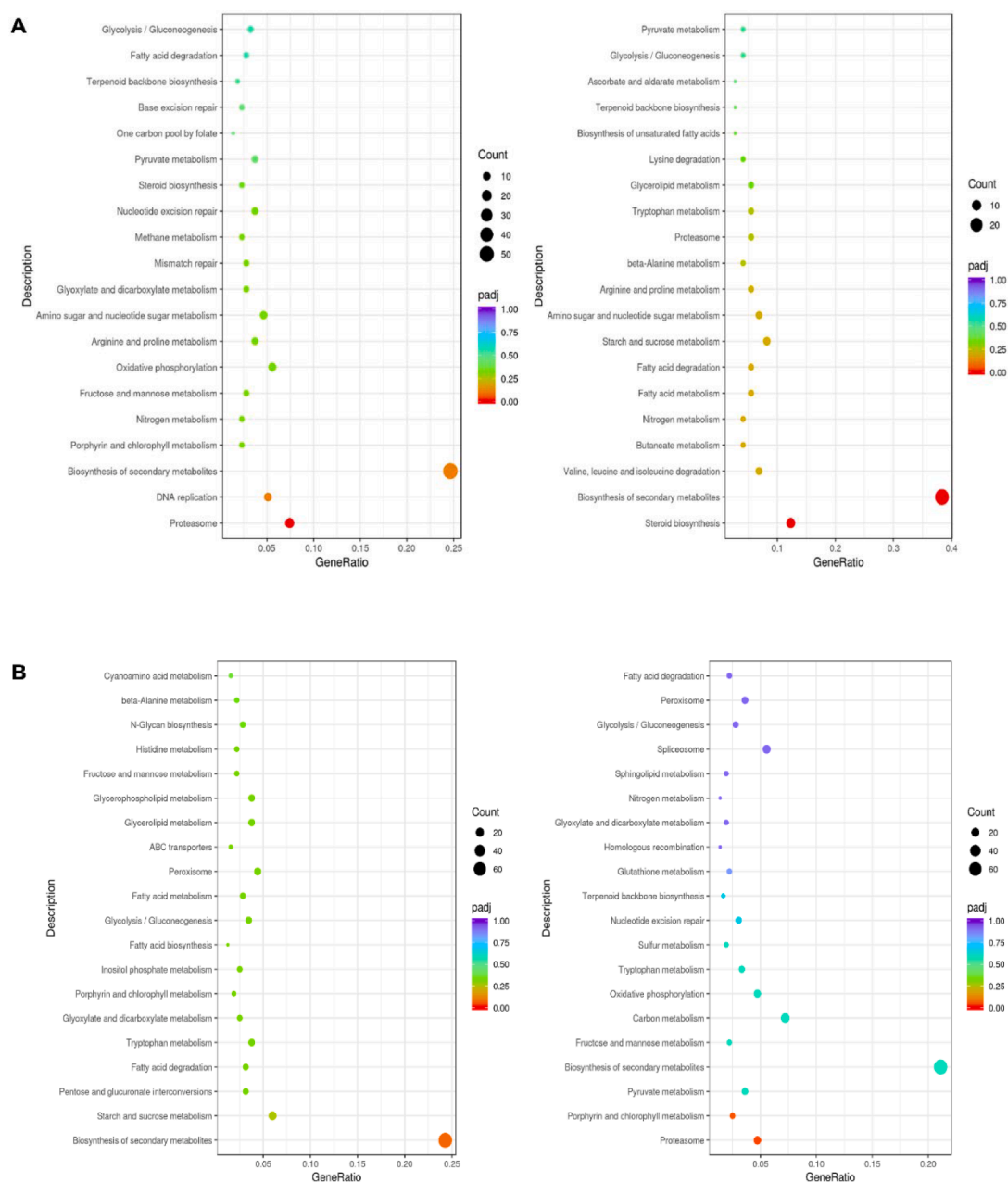
Fig. 4. KEGG enrichment analysis of DEGs in P1 vs CK group (left) and P2 vs CK group (right). (A)10 d, (B)20 d, (C)30 d. CK: Control; P1:0.02 mm PE; P2:0.05 mm PE.
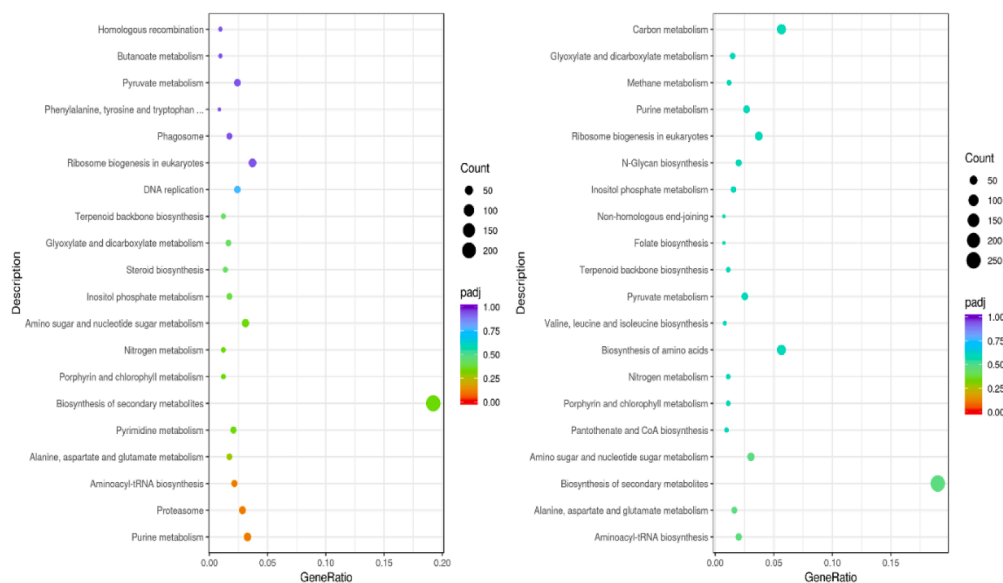
Fig. 4. (*continued*).

P. eryngii lignification, RNA-seq analysis was conducted periodically on the stipes. In combination with previous studies on lignin and enzyme activity, 10 d, 20 d and 30 d samples were selected for Illumina deep sequencing, in which P1 represents 0.02 mm PE treatment group and P2 represents 0.05 mm PE treatment group. Each group was assigned to three biological replications, such as P1_10_1 representing 10 d for 0.02 mm PE treated group samples. All samples showed good sequencing quality and correlated well with biological replicates (Table S1, Table S2, Figure S1). The number of differential genes tended to increase in the PE vs CK group as the storage time increased. Meanwhile, from 20 d onward, the P2 vs CK group had more DEGs than the P1 vs CK group (Figure S2).

The DEGs in the two comparison groups were annotated with GO enrichment analysis to describe the functions of DEGs in terms of biological processes (BP), cell components (CC), and molecular functions (MF) (Figure S3). In BP category, the "Metabolic processes" of the two packaging treatments were abundant, indicating the catabolism of mycelium during storage was influenced by PE materials, such as phenylpropane metabolic pathway. In CC, DEGs was mainly involved in "Organelle envelope" and "Membrane part", which indicated that PE could alleviate the damage of cell membrane caused by cold injury. In MF, "Oxidoreductase activity" appeared frequently, which indicated that PE could regulate the quality change of *P. eryngii* by catalyzing and activating various enzymes.

We further analyzed the function of DEGs by KEGG enrichment (Fig. 4). At 10 d, the enriched pathway of DEGs between PE treated group and CK group was mainly related to biosynthesis of secondary metabolism (abp01110). In addition, DEGs from P2 vs CK group were found to be enriched in steroid biosynthesis (abp00100). At 20 d, DEGs were involved in the biosynthesis of secondary metabolites and peroxisome (abp04146). At 30d, the distribution pathways of DEGs include phenylalanine, tyrosine and tryptophan biosynthesis (abp00400) and phenylalanine metabolism (abp00360). The results showed that PE was involved in the regulation of secondary metabolism of *P. eryngii*, and controls the amino acid activation and phenylalanine synthesis, which includes phenylpropanoid metabolites like lignin.

In addition, DEGs in P1 vs CK group and P2 vs CK group were involved in glyoxylate and dicarboxylate metabolism (abp00630), pyruvate metabolism (abp00620) and glycolysis/gluconeogenesis (abp00010). This suggests that PE packaging might interfere with glyoxylate cycle, redox and respiratory metabolism in *P. eryngii*.

3.5. Expression of DEGs related to lignin synthesis and decomposition

To explore the effect of PE on the expression levels of genes related to the lignification process, a certain number of DEGs were identified and their expression patterns were analyzed at each period separately (Fig. 5A).

At 10 d, P1 treatment group upregulated five versatile phase peroxidase and laccase related genes: *versatile liquid phase peroxidase-1 (VPL-1)*, *VPL-2, Laccase-2, Laccase-1, Laccase-2*. Ca^{2+} metabolism related genes *Pleery1|1424046,* Pleery1|1447532 and PCD protein related genes *Pleery1|1501548, Pleery1|1442143* were up-regulated. *POD-2* and *4-CL-1* were down-regulated. Most of the above genes were also expressed in P2 group. In addition, P2 group upregulated the expression of two kinds of versatile peroxidase related genes: *VPL-1,* and the laccase related gene *Laccase-2*.

At 20 d, P1 treatment group upregulated the expression of 9 genes related to ligninolytic enzymes, including *VPL-1*, *versatile solid phase peroxidase-1(VSL-1)*, *LAC-1* and *LAC-2*. Among the downregulated genes were three genes each annotated to lignin synthase and Ca^{2+} metabolism. In addition, the expression of five PCD proteins and key enzyme RNase related genes were down regulated. The gene expression pattern of P2 group was similar, and the additional up-regulated gene *Pleery1 | 1,394,244* was related to *LAC-1*.

At 30 d, 20 relevant DEGs were screened, most of which were the same as at 20 d. The trends were generally consistent. However, the fold change was further expanded. For example, in P1 group, the gene *LAC-2* had a fold change of 1.43 and only 0.37 at 20 d. In P2 group, *VPL-1* had a fold change of 2.11, a significant increase from 0.54 on 20 d. Compared with 0.01 at 20 d, the folding difference of *VPL-2* reached 1.10. Moreover, the two groups of PE packaging further inhibited the expression of Ca^{2+} channel metabolism gene and PCD protein related gene. Details of DEGs related to lignification process during storage are shown in Table S3.

Based on the above analysis, we selected 10 genes and verified the accuracy of RNA-seq data by qRT-PCR. As shown in Fig. 5(B), the results are basically consistent with high-throughput sequencing data, which confirms the reliability of sequencing data.

3.6. Distribution of lignin in cell wall

To further explore the mechanism of PE packaging inhibition of lignification, CRM was used to investigate the dynamic changes of lignin
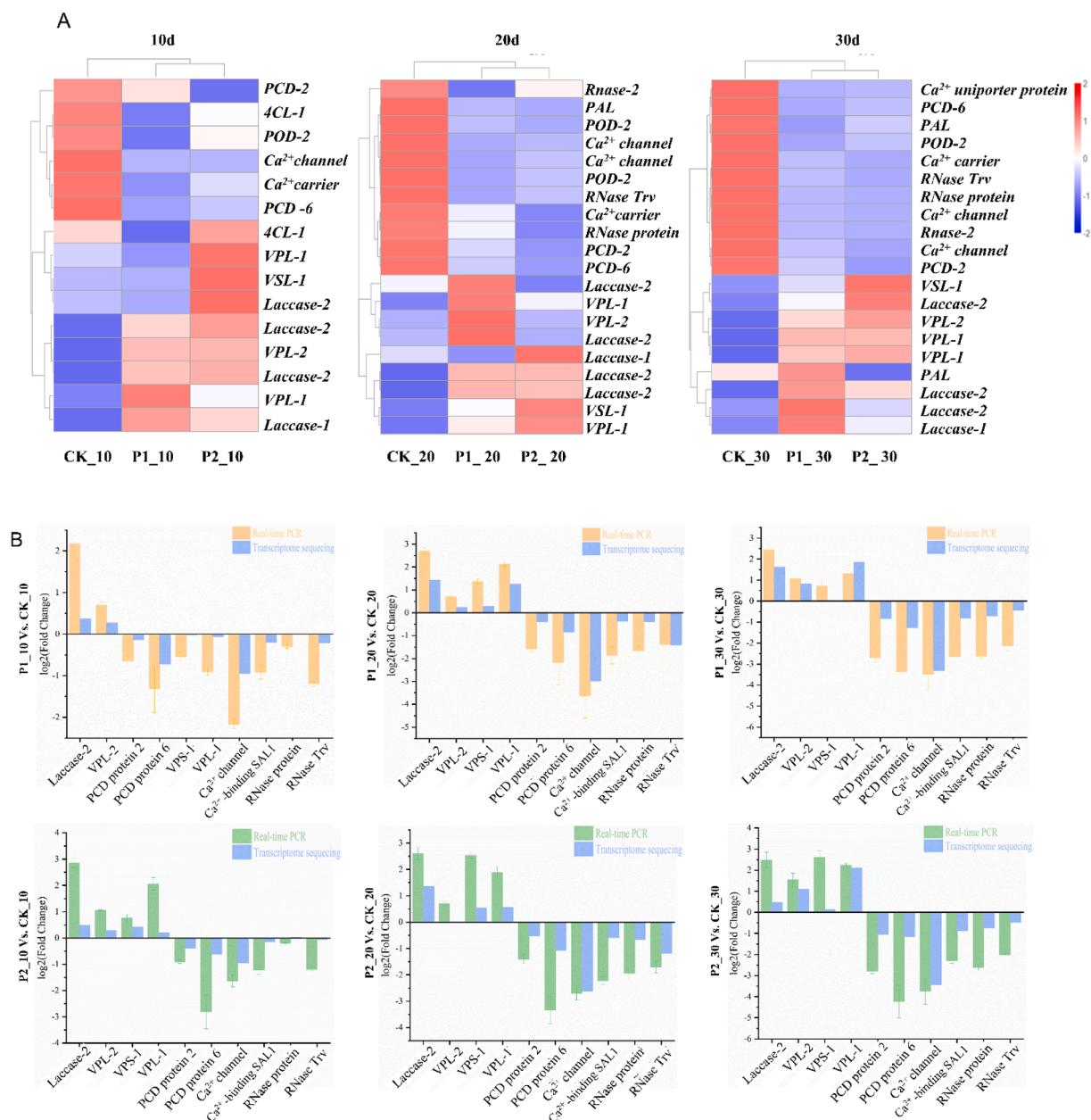
Fig. 5. (A)The expression pattern of DEGs related to lignification process during storage. The rows in heat map represent gene names and the columns represent samples. The color of heat map cell indicates the gene expression level in different samples. The relative expression level was calculated using log2 (FPKM + 1). (B) Validation of DEG by qRT-PCR.

in the mushroom stalk tissues of *P. eryngii* (Fig. 6). After spectral pre-treatment, the wave number range of 1550–1700 cm^{-1} was selected for integration to visualize the lignin (W. N. Huang et al., 2019).

For fresh *P. eryngii* (0 d), only low-intensity lignin signals distributed uniformly in the cell wall were observed. After 10 d, the area of lignin signal peak was enlarged in CK group and the signal intensity in local area reached 6000. In contrast, the signal area and intensity of PE group decreased. From 20 d to 30 d, cell wall lignin was deposited in the CK group, and there were obvious lignin signal intensity bands, some of which exceeded 8000 (Fig. 6A). At the same time, the lignin signal was weakened in PE group at 20 d, and the lignin deposition was delayed at 30 d. 0.05 mm PE group prevented the formation of lignin band signal at 30 d (Fig. 6C), and the lignin signal in visual field was lower than that in control group and 0.02 mm PE Group.

4. Discussion

By observing the phenotype of *P. eryngii* under different treatments during storage, PE material effectively inhibited the deterioration of postharvest appearance and tissue of *P. eryngii*. Compared with 0.02 mm PE, 0.05 mm PE played a more effective role in alleviating quality deterioration. In CK group, there were two peaks of firmness and lignin content in 10 d and 20 d. The fluctuation of lignin content during storage was consistent with previous reports (Wang et al., 2019). It was speculated that low temperature (4 °C) could affect firmness by affecting lignification degree of *P. eryngii*. The rise of firmness in the previous period may result from lignin deposition, tissue fibrosis and lignification in *P. eryngii*. Whereas the drastic decrease of firmness at the late stage of storage originated from cellulose degradation in the cell wall and tissue softening in *P. eryngii*. However, PE packaging can maintain the firmness of *P. eryngii* and inhibit its postharvest senescence progress.
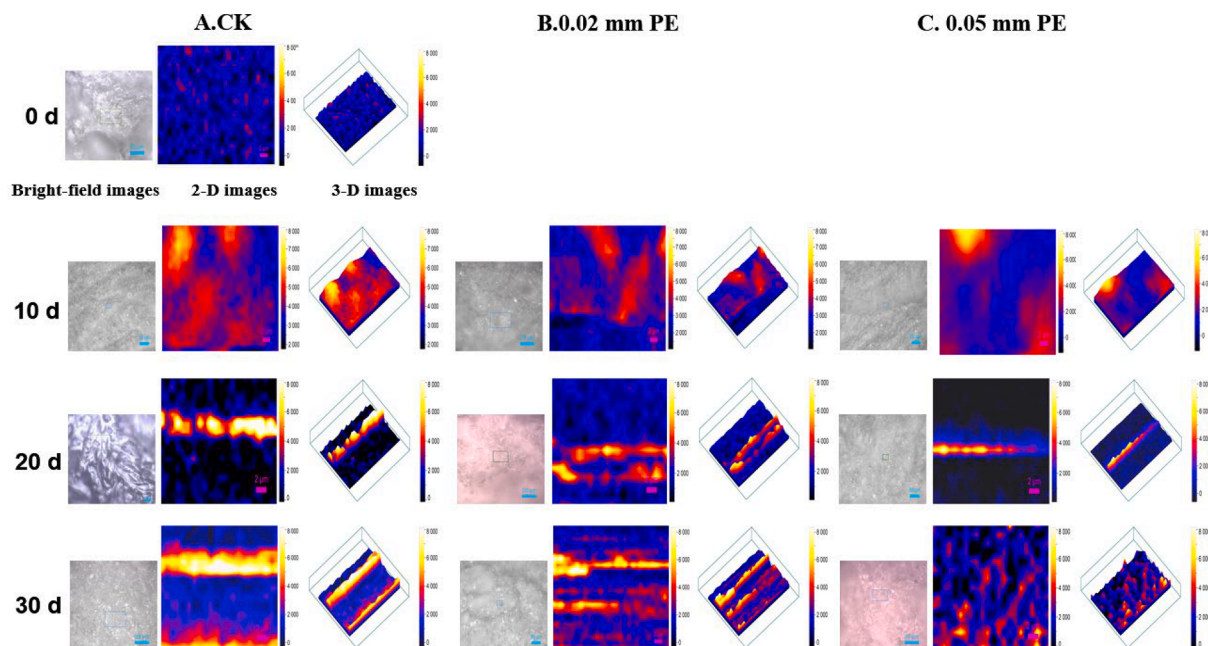
Fig. 6. Bright field images and 2-D and 3-D Raman images of lignin distribution in the cell wall of *P. eryngii* (1550–1700 cm^{-1}) (A) CK, (B) 0.02 mm PE, (C) 0.05 mm PE.

Postharvest lignification is an abnormal accumulation of lignin caused by external defense reaction such as low temperature or mechanical damage. Lignin is one of the most important secondary metabolites produced by plant phenylalanine / tyrosine metabolic pathway (Liu et al., 2018). During storage, three peaks of lignin content appeared in the CK group, parallel to two significant peaks of hardness index at 10 and 20 d, confirming that the increase in lignin led to lignification and increased the firmness of *P. eryngii*. At the same time, lignin content of PE group was significantly reduced at 10 d, 20 d and 30 d, suggesting that these are key time points for the differential expression of lignin-related genes. Therefore, we selected these time points for RNA-seq to analyze the molecular pathway of PE inhibiting *P. eryngii* lignification.

PAL (EC 4.3.1.5) is a key starting enzyme in the lignin biosynthesis pathway, catalyzing metabolic process from L-Phenylalanine to cinnamic acid. 4CL (EC 6.2.1.12) is a key enzyme in the phenylpropanoid pathway of plants and can catalyze the formation of diverse biomacromolecules such as lignin precursors and flavonoids (Lavhale et al., 2021). POD (EC 1.11.1.7) mediates the final step of lignin biosynthesis by catalyzing the polymerization of lignin precursors in hydrogen peroxide to produce lignin (Jin et al., 2021).In this study, PAL and 4-CL activities of *P. eryngii* increased in different degrees during low temperature. The lignin content reached its peak at 10 d, 20 d and 30 d, which coincided with peak time of lignin content. The results showed that PAL and 4-CL synthesized and transformed phenolic substrates through the phenol-propane pathway under the stimulation of cold damage in *P. eryngii*, leading to multiple lignification during storage (Wang et al., 2020). PE packaging reduced PAL and 4-CL activities, thereby preventing the conversion of L-phenylalanine and synthesis of lignin precursors. This resulted in the suppression of lignification phenomena under PE treatment, which restrained the rapid rise in firmness and delayed the decline in springiness. Transcriptome analysis revealed that *4CL-1*, *POD-2*, *Laccase-1*, and *Laccase-2* were regulated at 10 d, and the expression patterns were largely consistent with the above enzyme levels. Similar trends were observed in the transcriptome DEGs at 20 d, 30 d, implying that the expression and transcript levels of these target genes may have some potential relationship with the corresponding enzyme activities. However, some genes were transcriptionally or translationally susceptible and lost the association with enzyme activity,

so further critical review is needed to verify the specific relationship.

Laccase (EC1.10.3.2) is a multi-copper oxidase which originally found in the resin of *Rhus vernicifera* and widely distributed in fungi and plants (Geniselli da Silva, 2021). For fungi, laccase plays an important role in the metabolic process of lignin depolymerization and catabolism by producing cationic radicals in the substrate to oxidize the phenolic subunits of lignin, leading to subsequent lipid or aromatic bond breakage and lignin depolymerization (Boruah et al., 2020). There was no significant difference in laccase activity between treatments in the initial stage (Fig. 3). However, starting from 10 d, the laccase activity of PE group increased continuously, which indicated that the organism could synthesize more laccase to deal with the adversity of lignin content increasing. According to the changes of lignin content in different treatments, activating laccase is one of the crucial ways to reduce lignin content and prevent lignification.

GO analysis indicated that secondary metabolic processes of mycelia such as phenylpropanoid metabolic pathway were affected by PE materials, and the damage of cell membrane or cell structure induced by low temperature was also alleviated. PE can utilize various enzymes to comprehensively regulate *P. eryngii* quality, presumably including enzymes critical to lignin synthesis. The KEGG results further suggest that PE is involved in the regulation of secondary metabolism in A. alba, controlling the activation of some amino acids and the synthesis of L-phenylalanine, including lignin and phenyl propane and other phenyl propane metabolites Wang et al. (2021) found that during lignin degradation by *Phanerochaete sordida* YK624, genes involved in energy metabolic pathways such as TCA cycle, lipid metabolism, carbon metabolism and glycolysis were upregulated. PE may interfere with lignin-decomposing enzymes and energy supply through secondary metabolism and energy metabolism.

As with Laccase, VP (EC 1.111.16, isozymes VPL and VPS) is considered to play a crucial role in the decomposition of lignin by fungi (Hernandez-Bueno et al., 2021). In this study, we analyzed DEGs in the PE treated group versus CK group at three time points and screened out important genes regarding lignin synthesis and decomposition. The expression of genes related to LAC-1, LAC −2, VPL-1, VPL-2 and VPS-1was up-regulated in PE treated group at different storage periods. This suggests that there was no surge in lignin content in the PE-treated

group under low temperature storage, probably due to the high expression of these ligninolytic enzymes activated by the PE material. Meanwhile, the expression of lignin synthase such as 4CL-1, POD-2 and PAL were intervened by PE treatment. Significantly, P2 group was more active than P1 group in inhibiting lignin synthase expression, which explained the lower lignin content in P2 group. Thus, the activity of ligninolytic enzymes, the expression pattern of lignin synthase in the phenyl propane metabolic pathway and the metabolic pathway showed consistency with the transcriptional level. However, some of the enzyme activities (substrate to product conversion) still need further study to elucidate.

In addition to the phenylpropane pathway, ROS, Ca^{2+} and PCD in mitochondria also influence the process of cell lignification·H_2O_2 is regarded as one of the main ROS involved in the lignification process. It is involved in the oxidative polymerization of lignin by sinapyl alcohol, coumaryl and coniferyl, thus catalyzing the lignification process (Denness et al., 2011). The differentiation of xylem is a typical PCD process, intracellular Ca^{2+} accumulation could alter the mitochondrial membrane potential and release pro apoptotic proteins, leading to PCD (Yin et al., 2022). The present study showed that PE packaging could effectively reduce the increase of H_2O_2 (Fig. 2D). Transcriptional data showed that PE packaging inhibited the expression of PCD, Ca^{2+}-dependent channel and transporter protein-related genes, and the degree of inhibition was proportional to storage time. Moreover, the expression of RNase related genes was down regulated to varying degrees, starting from 20 d. These results suggested that PE packaging could delay the PCD process by maintaining mitochondrial Ca^{2+} homeostasis and inhibiting mitochondrial ROS accumulation, and finally inhibit lignification (Shi et al., 2020). However, more comprehensive monitoring of reactive oxygen species and PCD in mitochondria is needed to confirm.

At present, most studies on lignification are based on the physiological indexes and molecular biology of tissue homogenate, the visualization of lignin changes with time and space on cell level will promote the understanding of PE packaging inhibiting lignification. CRM has been used for the visualization of components in horticultural products because of its label-free, short time, good stability and high spatial resolution (Khodabakhshian, 2019). In this study, Raman signals of lignin characteristic bands in the spectral range of 1550–1700 cm^{-1} were observed. The results showed that the lignin in the cell wall of *P. eryngii* was deposited with time and accompanied by high-strength band lignin peak. Before 20 d, the lignin distribution pattern of PE group was like that of CK group, but the signal intensity and peak area decreased significantly. At 30 d, lignin in 0.05 mm PE group was scattered and the signal intensity was lower than CK group. The results showed that PE packaging, especially 0.05 mm PE, could delay the deposition of lignin in *P. eryngii* effectively and reduce the distribution in cell wall.

In addition, we found differences in gene regulation by different thicknesses of PE materials, which we speculate may be due to differences in respiratory metabolism of different thicknesses of *P. eryngii*, the exact mechanism of which needs to be further investigated. We will continue to observe more packaging materials (nano, edible film) from the transcriptome perspective on the quality of *P. eryngii* to improve the relevant molecular mechanisms. On this basis, the targeted gene editing strategy may provide a new idea for the improvement of food mushroom varieties (Kim and Kim, 2016; Wang et al., 2021). Meanwhile, we made a preliminary exploration on the application of CRM to the visualization of lignin cell level in *P. eryngii*. More lignin characteristic bands and other components of the cell wall such as cellulose will be the focus in the future.

CRediT authorship contribution statement

Wancong Yu: Conceptualization, Methodology, Writing – original draft. **Shihao Li:** Conceptualization, Methodology, Writing – original draft. **Bowen Zheng:** Software. **Yuqi Wang:** . **Yue Yu:** Validation. **Yumeng Wang:** . **Xu Zheng:** . **Jiping Liu:** Writing – review & editing. **Zhijun Zhang:** Supervision, Writing – review & editing. **Zhaohui Xue:** Supervision, Writing – review & editing.

Declaration of Competing Interest

The authors declare that they have no known competing financial interests or personal relationships that could have appeared to influence the work reported in this paper.

Acknowledgement

References

Boruah, P., Sarmah, P., Das, P. K., & Goswami, T. (2020). Exploring the lignolytic potential of a new laccase producing strain Kocuria sp. PBS-1 and its application in bamboo pulp bleaching (vol 143, 104726, 2019). *International Biodeterioration & Biodegradation, 155*. https://doi.org/ARTN 105110 10.1016/j.ibiod.2020.105110.

Cesarino, I. (2019). Structural features and regulation of lignin deposited upon biotic and abiotic stresses. *Current Opinion in Biotechnology, 56*, 209–214. https://doi.org/10.1016/j.copbio.2018.12.012

Chylinska, M., Szymanska-Chargot, M., Derylo, K., Tchorzewska, D., & Zdunek, A. (2017). Changing of biochemical parameters and cell wall polysaccharides distribution during physiological development of tomato fruit. *Plant Physiology and Biochemistry, 119*, 328–337. https://doi.org/10.1016/j.plaphy.2017.09.010

Denness, L., McKenna, J. F., Segonzac, C., Wormit, A., Madhou, P., Bennett, M., … Hamann, T. (2011). Cell Wall Damage-Induced Lignin Biosynthesis Is Regulated by a Reactive Oxygen Species- and Jasmonic Acid-Dependent Process in Arabidopsis. *Plant Physiology, 156*(3), 1364–1374. https://doi.org/10.1104/pp.111.175737

Du, F., Zou, Y., Hu, Q., Zhang, H., & Ye, D. (2020). Comparative transcriptomic analysis reveals molecular processes involved in pileus morphogenesis in Pleurotus eryngii under different light conditions. *Genomics, 112*(2), 1707–1715. https://doi.org/10.1016/j.ygeno.2019.09.014

Fallah-Joshaqani, S., Hamdami, N., & Keramat, J. (2021). Qualitative attributes of button mushroom (Agaricus bisporus) frozen under high voltage electrostatic field. *Journal of Food Engineering, 293*, 110384. https://doi.org/10.1016/j.jfoodeng.2020.110384

Geniselli da Silva, V. (2021). Laccases and ionic liquids as an alternative method for lignin depolymerization: A review. *Bioresource Technology Reports, 16*. https://doi.org/10.1016/j.biteb.2021.100824

Hassan, A., Pariatamby, A., Ossai, I. C., & Hamid, F. S. (2020). Bioaugmentation assisted mycoremediation of heavy metal and/metalloid landfill contaminated soil using consortia of filamentous fungi. *Biochemical Engineering Journal, 157*, 107550. https://doi.org/10.1016/j.bej.2020.107550

Hernandez-Bueno, N. S., Suarez-Rodriguez, R., Balcazar-Lopez, E., Folch-Mallol, J. L., Ramirez-Trujillo, J. A., & Iturriaga, G. (2021). A Versatile Peroxidase from the Fungus Bjerkandera adusta Confers Abiotic Stress Tolerance in Transgenic Tobacco Plants. *Plants (Basel), 10*(5). https://doi.org/10.3390/plants10050859

Hou, D., Lu, H., Zhao, Z., Pei, J., Yang, H., Wu, A., … Lin, X. (2022). Integrative transcriptomic and metabolomic data provide insights into gene networks associated with lignification in postharvest Lei bamboo shoots under low temperature. *Food Chem, 368*, Article 130822. https://doi.org/10.1016/j.foodchem.2021.130822

Huang, W., Zhu, N., Zhu, C., Wu, D., & Chen, K. (2019). Morphology and cell wall composition changes in lignified cells from loquat fruit during postharvest storage. *Postharvest Biology and Technology, 157*. https://doi.org/10.1016/j.postharvbio.2019.110975

Huang, W. N., Zhu, N., Zhu, C. Q., Wu, D., & Chen, K. S. (2019). Morphology and cell wall composition changes in lignified cells from loquat fruit during postharvest storage. *Postharvest Biology and Technology, 157*, 110975. https://doi.org/10.1016/j.postharvbio.2019.110975

Jiang, T. J., Jahangir, M. M., Wang, Q. S., & Ying, T. J. (2010). Accumulation of Lignin and Malondialdehyde in Relation to Quality Changes of Button Mushrooms (Agaricus bisporus) Stored in Modified Atmosphere. *Food Science and Technology International, 16*(3), 217–224. https://doi.org/10.1177/1082013209353840

Jin, M. J., Jiao, J. Q., Zhao, Q. X., Ban, Q. Y., Gao, M., Suo, J. T., … Rao, J. P. (2021). Dose effect of exogenous abscisic acid on controlling lignification of postharvest kiwifruit (Actinidia chinensis cv. hongyang). *Food Control, 124*, 107911. https://doi.org/10.1016/j.foodcont.2021.107911

Khodabakhshian, R. (2019). Feasibility of using Raman spectroscopy for detection of tannin changes in pomegranate fruits during maturity. *Scientia Horticulturae, 257*, 108670. https://doi.org/10.1016/j.scienta.2019.108670

Kim, J., & Kim, J. S. (2016). Bypassing GMO regulations with CRISPR gene editing. *Nature Biotechnology, 34*(10), 1014–1015. https://doi.org/10.1038/nbt.3680

Kleftaki, S. A., Simati, S., Amerikanou, C., Gioxari, A., Tzavara, C., Zervakis, G. I., … Kaliora, A. C. (2022). Pleurotus eryngii improves postprandial glycaemia, hunger

and fullness perception, and enhances ghrelin suppression in people with metabolically unhealthy obesity. *Pharmacological Research, 175*, 105979. https://doi.org/10.1016/j.phrs.2021.105979

Lavhale, S. G., Joshi, R. S., Kumar, Y., & Giri, A. P. (2021). Functional insights into two Ocimum kilimandscharicum 4-coumarate-CoA ligases involved in phenylpropanoid biosynthesis. *Int J Biol Macromol, 181*, 202–210. https://doi.org/10.1016/j.ijbiomac.2021.03.129

Li, Q., Huang, W., Xiong, C., & Zhao, J. (2018). Transcriptome analysis reveals the role of nitric oxide in Pleurotus eryngii responses to Cd2+ stress. *Chemosphere, 201*, 294–302. https://doi.org/10.1016/j.chemosphere.2018.03.011

Li, Y. E., Wang, H. H., Zhang, W. B., Wu, H. N., & Wang, Z. (2021). Evaluation of nutrition components in Lanzhou lily bulb by confocal Raman microscopy. *Spectrochimica Acta Part a-Molecular and Biomolecular Spectroscopy, 244*, 150-154. https://doi.org/ARTN 118837 10.1016/j.saa.2020.118837.

Liu, Q., Luo, L., & Zheng, L. (2018). Lignins: Biosynthesis and Biological Functions in Plants. *International Journal of Molecular Sciences, 19*(2). https://doi.org/10.3390/ijms19020335

Livak, K. J., & Schmittgen, T. D. (2001). Analysis of relative gene expression data using real-time quantitative PCR and the 2(-Delta Delta C(T)) Method. *Methods, 25*(4), 402–408. https://doi.org/10.1006/meth.2001.1262

Min, T., Niu, L. F., Feng, X. Y., Yi, Y., Wang, L. M., Zhao, Y., & Wang, H. X. (2021). The effects of different temperatures on the storage characteristics of lotus (Nelumbo nucifera G.) root. *Food Chem, 348*, Article 129109. https://doi.org/10.1016/j.foodchem.2021.129109

Nie, X. B., Zhang, R. C., Cheng, L. L., Li, S. L., Zhao, X. R., & Chen, X. M. (2020). Combining the biocontrol yeast Pichia kluyveri with UV-C treatment to control postharvest decay of king oyster mushrooms (Pleurotus eryngii) caused by Lactococcus lactis subsp. lactis. *Biological Control, 149*, 104327. https://doi.org/10.1016/j.biocontrol.2020.104327

Shekari, A., Hassani, R. N., & Aghdam, M. S. (2021). Exogenous application of GABA retards cap browning in Agaricus bisporus and its possible mechanism. *Postharvest Biology and Technology, 174*, 111434. https://doi.org/10.1016/j.postharvbio.2020.111434

Shi, C., Wu, Y. Y., Fang, D. L., Ma, N., Mariga, A. M., Hu, Q. H., & Yang, W. J. (2020). Nanocomposite packaging regulates extracellular ATP and programed cell death in edible mushroom (Flammulina velutipes). *Food Chemistry, 309*, 125702. https://doi.org/10.1016/j.foodchem.2019.125702

Sun, M., Yang, X. L., Zhu, Z. P., Xu, Q. Y., Wu, K. X., Kang, Y. J., … Xiong, A. S. (2021). Comparative transcriptome analysis provides insight into cold storage suppressing lignin accumulation of postharvest okra (Abelmoschus esculentus L.) during cold storage. *Plant Physiol Biochem, 167*, 49–67. https://doi.org/10.1016/j.plaphy.2021.07.029

Suo, J. T., Li, H., Ban, Q. Y., Han, Y., Meng, K., Jin, M. J., … Rao, J. P. (2018). Characteristics of chilling injury-induced lignification in kiwifruit with different sensitivities to low temperatures. *Postharvest Biology and Technology, 135*, 8–18. https://doi.org/10.1016/j.postharvbio.2017.08.020

Szymanska-Chargot, M., Chylinska, M., Pieczywek, P. M., Rosch, P., Schmitt, M., Popp, J., & Zdunek, A. (2016). Raman imaging of changes in the polysaccharides distribution in the cell wall during apple fruit development and senescence. *Planta, 243*(4), 935–945. https://doi.org/10.1007/s00425-015-2456-4

Teniou, S., Bensegueni, A., Hybertson, B. M., Gao, B., Bose, S. K., McCord, J. M., … Hininger-Favier, I. (2022). Biodriven investigation of the wild edible mushroom Pleurotus eryngii revealing unique properties as functional food. *Journal of Functional Foods, 89*. https://doi.org/10.1016/j.jff.2022.104965

Wang, J., Suzuki, T., Mori, T., Yin, R., Dohra, H., Kawagishi, H., & Hirai, H. (2021). Transcriptomics analysis reveals the high biodegradation efficiency of white-rot fungus Phanerochaete sordida YK-624 on native lignin. *J Biosci Bioeng, 132*(3), 253–257. https://doi.org/10.1016/j.jbiosc.2021.05.009

Wang, T. L., Yue, S., Jin, Y. T., Wei, H., & Lu, L. (2021). Advances allowing feasible pyrG gene editing by a CRISPR-Cas9 system for the edible mushroom Pleurotus eryngii. *Fungal Genetics and Biology, 147*, 103509. https://doi.org/10.1016/j.fgb.2020.103509

Wang, Y., Mo, Y. L., Li, D. Q., Xiang, C. Y., Jiang, Z. D., & Wang, J. (2019). The main factors inducing postharvest lignification in king oyster mushrooms (Pleurotus eryngii): Wounding and ROS-mediated senescence. *Food Chemistry, 301*, 125224. https://doi.org/10.1016/j.foodchem.2019.125224

Wang, Y., Xiang, C., Li, D., Du, M., Mo, Y., Jiang, Z., & Wang, J. (2020). Identification of key genes involved in the two lignifications in stored king oyster mushrooms (Pleurotus eryngii) and their expression features. *Postharvest Biology and Technology, 169*. https://doi.org/10.1016/j.postharvbio.2020.111289

Wang, Y., Xiang, C. Y., Li, D. Q., Du, M. R., Mo, Y. L., Jiang, Z. D., & Wang, J. (2020). Identification of key genes involved in the two lignifications in stored king oyster mushrooms (Pleurotus eryngii) and their expression features. *Postharvest Biology and Technology, 169*, 111289. https://doi.org/10.1016/j.postharvbio.2020.111289

Wen, M., Wang, H., Chen, Y., Jiang, Y., Chen, F., & Luo, Z. (2020). Inhibition effect of super atmospheric O2 packaging on H2O2-production and the key enzymes of ligin biosynthesis in fresh-cut Chinese cabbage. *Postharvest Biology and Technology, 159*. https://doi.org/10.1016/j.postharvbio.2019.111027

Wu, X., Zhang, Z., Sun, M., An, X., Qi, Y., Zhao, S., … Wang, H. (2021). Comparative transcriptome profiling provides insights into endocarp lignification of walnut (Juglans Regia L.). *Scientia Horticulturae, 282*. https://doi.org/10.1016/j.scienta.2021.110030

Xu, F., Chen, P., Li, H., Qiao, S., Wang, J., Wang, Y., … Xu, H. (2021). Comparative transcriptome analysis reveals the differential response to cadmium stress of two Pleurotus fungi: Pleurotus cornucopiae and Pleurotus ostreatus. *Journal of Hazardous Materials, 416*, Article 125814. https://doi.org/10.1016/j.jhazmat.2021.125814

Yin, J. J., Xiong, J., Xu, L. T., Chen, W. W., & Li, W. T. (2022). Recent advances in plant immunity with cell death: A review. *Journal of Integrative Agriculture, 21*(3), 610–620. https://doi.org/10.1016/S2095-3119(21)63728-0

Zhang, C., Song, X. L., Cui, W. J., & Yang, Q. H. (2021). Antioxidant and anti-ageing effects of enzymatic polysaccharide from Pleurotus eryngii residue. *International Journal of Biological Macromolecules, 173*, 341–350. https://doi.org/10.1016/j.ijbiomac.2021.01.030

Zhang, W. L., Jiang, H. T., Cao, J. K., & Jiang, W. B. (2021). Advances in biochemical mechanisms and control technologies to treat chilling injury in postharvest fruits and vegetables. *Trends in Food Science & Technology, 113*, 355–365. https://doi.org/10.1016/j.tifs.2021.05.009

Zhuo, R., & Fan, F. (2021). A comprehensive insight into the application of white rot fungi and their lignocellulolytic enzymes in the removal of organic pollutants. *Sci Total Environ, 778*, Article 146132. https://doi.org/10.1016/j.scitotenv.2021.146132

Zuo, C. Z., Hu, Q. H., Su, A. X., Xu, H., Li, X. T., Mariga, A. M., & Yang, W. J. (2021). Nanocomposite packaging delays lignification of Flammulina velutipes by regulating phenylpropanoid pathway and mitochondrial reactive oxygen species metabolisms. *Postharvest Biology and Technology, 171*, 111360. https://doi.org/10.1016/j.postharvbio.2020.111360